Optimizing Gene Expression Programming to Predict Shear Capacity in Corrugated Web Steel Beams

Mazen Shrif [1] , Zaid A. Al-Sadoon [1*] , Samer Barakat [1] , Ahed Habib [2] , Omar Mostafa [1]

[1] *Department of Civil and Environmental Engineering, College of Engineering, University of Sharjah, Sharjah, United Arab Emirates.*

[2] *Research Institute of Sciences and Engineering, University of Sharjah, Sharjah, United Arab Emirates.*

Abstract

Corrugated web steel systems, such as corrugated web girders (CWG) and beams (CWSB), have the potential to influence the modern construction industry due to their unique properties, including enhanced shear strength and reduced necessity for transverse stiffeners. Nevertheless, the lack of a rapid and accurate design approach still limits its wide applications. Recently, gene expression programming (GEP) has been employed to predict the shear capacity of cold-formed steel channels, demonstrating superior predictive accuracy and compliance with established standards. This study applies GEP to predict the shear capacity of sinusoidal CWSBs and optimizes its predictive performance by employing a systematic grid search to explore combinations of chromosomes, head sizes, gene counts, and linking functions. The process involved testing 19 different parameter combinations and more than 60 developed models. The findings include the sensitivity of the model's performance to gene count and the critical role of the linking function. The optimal model in the study, GEP13, achieved R^2 of 0.95, an RMSE of 100.5, and an MAE of 86.6 in the testing dataset with 150 chromosomes, a head size of 12, and four genes using a multiplication linking function.

Keywords: Sinusoidal Steel Beam; SCWBS; ANN; Shear Strength Analysis; Network Topology; Predictive Modelling; Hyperparameter Optimization; Geometric Properties.

1. Introduction

Corrugated web steel systems, including corrugated web girders (CWG) and corrugated web steel beams (CWSB), have gained significant interest in the industrial and construction sectors. CWGs have been widely used in highway bridge projects, offering advantages such as reduced risk of damage during construction and operation [1, 2]. CWSBs, on the other hand, utilize thin corrugated webs and eliminate the need for transverse stiffeners while achieving remarkable shear strength capacities [3]. These innovations have led to the widespread recognition and integration of CWSBs in various construction projects, surpassing traditional welded sheet metal beams in terms of their potential benefits [4, 5]. This resurgence of interest in corrugated web steel systems has coincided with a growing trend in the structural engineering community towards embracing machine learning techniques for modeling and analysis. Researchers have proposed the use of machine learning algorithms, such as K-Nearest Neighbors, XGBoost, CatBoost, Random Forest, and support vector machines, to develop more accurate formulae for structural design and to enhance SHM for bridges [6–8].

Machine learning algorithms have been used to predict shear capacity, fundamental period, and deflection of structures, as well as to discriminate between healthy and non-healthy states of bridges [9, 10]. Additionally, machine

learning has been applied to estimate the plastic hinge length of reinforced concrete structural walls, providing better predictions than existing empirical equations [7, 10]. Artificial neural networks (ANNs) have also been used to predict the punching shear capacity of fiber-reinforced concrete (FRC) and fiber-reinforced polymer (FRP) concrete slabs [11, 12]. These studies demonstrate the increasing interest in and application of machine learning techniques in structural engineering.

Elamary & Taha [13] recently used Gaussian process regression to estimate steel beams' shear capacity with sinusoidal corrugated webs (SBCWs) and demonstrated its accurate performance. Ipek et al. [14] utilized gene expression programming (GEP) to develop models for predicting the shear capacity of cold-formed steel (CFS) channels with staggered slotted web perforations [14]. Hossain et al. [15] employed GEP to predict the compressive strength of fiber-reinforced geopolymer concrete (FRGC). Alabduljabbar et al. [16] focused on estimating the strength of ultra-high-performance concrete (UHPC) using GEP. These successful application of GEP, along with the possibility to estimate the shear behavior of corrugated web beams, represents a potential for solving more complex problems, particularly assessing the shear capacity of sinusoidal corrugated web beams (SCWBs), a notable research gap in the literature. Accordingly, this study aims to address this gap by developing and optimizing a GEP-based model to predict the shear capacity of SCWBs, establishing a novel approach in the field, and contributing to more accurate and efficient design procedures. The objectives extend to refining the GEP algorithm through training a variety of model cases and then selecting the best one. A variable importance and sensitivity analysis of structural parameters will be conducted to assess the impact of the parameters on the shear strength of SCWBs. The insights gained from this analysis are expected to align with mechanical behaviors observed in experimental studies and theoretical expectations. By contributing to more accurate, efficient, and reliable design procedures, this research not only fills a critical gap in the literature but also paves the way for more innovative applications of machine learning in civil engineering. The ultimate goal is to facilitate the adoption of SCWBs in broader construction practices, enabling engineers and designers to leverage their benefits in various projects, thereby promoting sustainability, cost-effectiveness, and architectural versatility in the construction industry.

2. Literature Review of Sinusoidal Corrugated Web Beams

Sinusoidal corrugated steel web (SCSW) stability design primarily relies on calculating the elastic shear buckling stress, and the design equation can be derived using the direct strength method. Elastic shear buckling in SCSW encompasses three main modes: local shear buckling (local buckling), global shear buckling (global buckling), and interactive shear buckling (interactive buckling). Interactive buckling represents a more intricate mode between local and global buckling [17]. The EN 1993-1-5 [18] calculated the local buckling stress as

$$\tau_l = \frac{k_L \pi^2 E}{12(1-v^2)} \left(\frac{t_w}{s}\right)^2 \tag{1}$$

K_L is the buckling coefficient, which depends on the boundary conditions and is a function of the panel aspect ratio (b/t), boundary support conditions, and plate height.

Figure 1 displays a sketch for the sinusoidal beam. The calculation of global buckling stress is simplified using the orthotropic plate buckling theory [19, 21]. Easley & McFarland [20] derived a simplified equation for the elastic global buckling shear stress of corrugated webs.
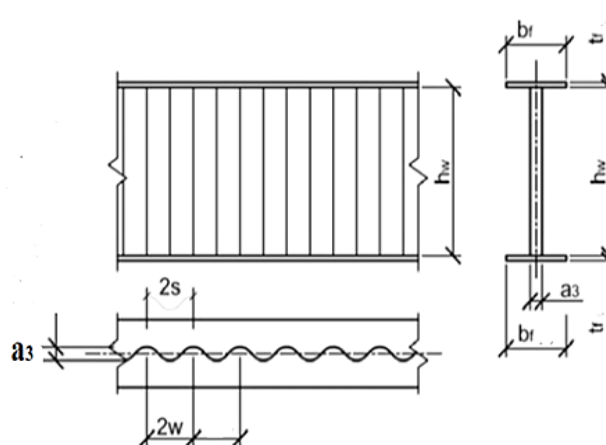

Figure 1. Geometric parameters of the sinusoidal corrugated web

$$\tau_G = K_G \frac{D_x^{\frac{1}{3}} D_y^{\frac{4}{3}}}{t_w H_w^2} \tag{2}$$

where

$$D_y = \frac{EI_y}{L_c} \tag{3}$$

$$D_x = \frac{Et_w^3}{12(1-v^2)}\frac{L_c}{S} \tag{4}$$

where I_y is the moment of inertia of one section of a corrugation wave about its neutral axis, S is the length of one sine wave. The studies performed by Pasternak & Branka [22] and have been proposed by Elkawas et al. [23] for the critical shear stress for local and global buckling for sinusoidally corrugated webs are as follows:

$$\tau_l = \left(5.34 + \frac{A_c S}{H_w t_w}\right)\frac{\pi^2 E}{12(1-v^2)}\left(\frac{t_w}{S}\right)^2 \tag{5}$$

$$\tau_G = 32.4 \frac{D_x^{\frac{1}{3}} D_y^{\frac{4}{3}}}{t_w H_w^2} \tag{6}$$

Although no specific independent calculation formula is provided, researchers widely believe that interactive buckling stress is related to local and global buckling stresses. Researchers conducted a study on the behavior of sinusoidal corrugated web girders under various loading conditions [21]. The study found that shear load capacity is significantly influenced by web geometry, specifically amplitude, wavelength, and thickness. Increasing amplitude and thickness leads to higher shear load capacity, while increasing wavelength reduces it. Various failure modes, such as web buckling, web crippling, and flange bending, were observed depending on the geometry and material properties of the corrugated web. Research on the impact of corrugated web geometry on I-beam behavior revealed similar outcomes to the previous study [24]. Also, Increased amplitude and thickness improve performance, while increased wavelength reduces load-carrying capacity. The experiments also identified failure modes influenced by web geometry, such as web buckling and flange bending.

3. Material and Methods

3.1. Gene Expression Programming

Gene expression programming is a scientific computer program that uses evolutionary algorithms to generate computer programs or models. The principles of nature inspire it and aim to create autonomous, problem-solving artificial systems. Its inception can be traced back to the pioneering work of Friedberg [25], which set the stage for the development of increasingly complex systems rooted in the concepts of natural evolution adapted to the computational world. Among these advancements, GEP emerges as the latest innovation in evolutionary computing [26]. GEP's evolution can be comprehended by comparing it with its predecessors, genetic algorithms (GAs) and genetic programming (GP). The introduction of GAs, based on a simplified interpretation of biological evolution, marked a significant milestone in the computational world [27].

Subsequently, GP, initially proposed by Cramer [28] and further refined by Koza [29], offered a distinctive approach by generating and genetically manipulating nonlinear structures of varying sizes and shapes to find solutions. In contrast to GAs that employ character strings (typically binary) to encode potential solutions, GP explore solution spaces by generating and manipulating tree structures [29]. The distinction lies in the nature of "individuals" representing solutions. In GAs, individuals correspond to chromosomes subject to mutation, crossover, and inversion, while in GP, individuals are tree-like structures upon which genetic operators, such as recombination, mutation, and permutation, directly act [29]. These operators play a fundamental role in shaping the genetic diversity critical for successful problem-solving. GEP bridges the gap between GAs and GP [26]. It shares with GP the capacity to evolve computer programs represented by diagram configurations. However, it introduces a significant addition compared to GP by encoding linear chromosomes of fixed length, often called the genotype, to represent expression trees, known as the phenotype [26, 30]. This innovation simplifies the complexity associated with GP and provides GEP with a notable advantage. One distinctive feature of GEP is the utilization of multiple genes within its chromosomes, each encoding a sub-program. This structural flexibility allows GEP to explore and operate complex solution spaces efficiently, enhancing its problem-solving capabilities. To facilitate the interpretation of genetic information within GEP, Ferreira [26] introduced the Karva language. This novel bilingual system bridges genotypes and phenotypes, enabling the seamless translation of complex expression trees into linear genetic representations. The Karva language permits the horizontal reading of expression trees in a vertical sequence, akin to reading text on a page. The fundamental genetic unit in GEP is the gene, which consists of a head and a tail of fixed length. The head contains symbols representing terminals and functions, while the tail only contains terminals. It is important to note that the variation in chromosome length in GEP arises from the open reading frames rather than the genes themselves. The genes collectively form the chromosomes, blueprints for evolving solution candidates [31]. Recently, GEP was applied to various civil engineering fields, given its comparable results against other common prediction techniques like ANN and polynomial regression [32, 33].

3.2. Data Collection and Methodology

This study develops a dataset of over 65 SCWBs collected from various experimental studies in the literature. The developed dataset contains a total of 6 geometrical and material input variables. These variables are the web depth (h_w), web thickness (t_w), the width of the longitudinal fold panel or the wavelength of the sinusoidal panel (a_1), corrugation depth or the wave amplitude (a_3), steel yield strength (τ_y), and the normalized elastic shear buckling strength (ρ). The experimental shear strength (V_{test}) of the SCWB was considered the only output variable in this study.

Table 1 lists the references used during data collection. Detailed information associated with each beam can be found in the appendix. Table 2 provides descriptive statistics of the prepared database, including the mean, standard deviation, minimum, first percentile (25%), median (50%), third percentile (75%), and maximum value. Once the database was developed, it was cleaned to eliminate outliers

Table 1. Shear strength of SCWB experimental testing data as obtained from the literature

Reference	Number of Specimens
SIN Technical Guideline (2018) [34]	6
Pasternak & Brańka (1999) [22]	3
Śledziewski & Górecki (2020) [36]	2
Pasternak & Kubieniec (2011) [35]	10
Górecki & Śledziewski (2022) [37]	6
Hannebauer (2007) [38]	13
Basiński (2018) [39]	10
Yan-lin et al. (2008) [40]	6
Nikoomanesh & Goudarzi (2021) [41]	9
Total	**65**

Table 2. Descriptive statistical analysis of the dataset

Parameter	Mean	Standard Deviation	Minimum	First Quartile	Median	Third Quartile	Maximum
Web depth h_w (mm)	341.2	250	1505	500	875	341.2	500
Web Thickness t_w (mm)	1.1	2	7	2.5	3	1.1	2.1
Wavelength a_1 (mm)	67.8	150	381	156	213	67.8	155
Corrugation depth a_3 (mm)	16.5	20	140	40	43	16.5	39.7
Steel yield strength τ_y (MPa)	61.3	225	434	302	355	61.3	247.5
Shear strength V_u (kN)	93.5	164.2	517.5	311.9	363.8	93.5	220.2

3.3. Model Development Strategy

To refine the gene expression programming (GEP) models for enhanced predictive accuracy, a systematic grid search was employed to navigate the hyperparameter space and mutable training for the same chosen parameters. Figure 2 shows the various stages of the GEP algorithm flowchart. This approach involved an extensive exploration of various combinations of chromosomes, head size, number of genes, and linking functions. The objective was to identify the configuration that maximizes the coefficient of determination (R^2) when tested against the data. Notably, 19 unique combinations of the most fitting parameters were simulated and tested. The database was randomly divided into 70% training, 15% validation, and 15% testing subsets during the model development stage. After that, the highest response in validation and testing was reported.

Table 3 displays models built on various parameters and functions. The models, GEP1 through GEP19, were tested with new data to assess their performance. The initial models, such as GEP1 with 50 chromosomes, a head size of 8, and 4 genes using an addition linking function, achieved an R^2 of 0.88. This strong performance set a high standard for subsequent models. However, variations in the model structure, as seen in GEP2 and GEP3, which had fewer genes, resulted in a decrease in R^2, indicating a sensitivity of model performance to the gene count. As the models evolved, there was a notable trend of increasing the number of chromosomes and adjusting the head size, significantly affecting model performance. Interestingly, changing the linking function from addition to multiplication in the same model configuration (GEP6) resulted in a lower R^2 of 0.86, suggesting that the choice of linking function is crucial and context-dependent. The grid search concluded in the development of GEP13, which exhibited an exceptional R^2 of 0.95, the highest among all models tested. This model stood out with its 150 chromosomes, head size of 12, and 4 genes utilizing a multiplication linking function. The optimized structure of GEP13 indicates that a higher number of chromosomes and a larger head size, when coupled with a multiplication linking function, can significantly enhance the model's predictive capability.
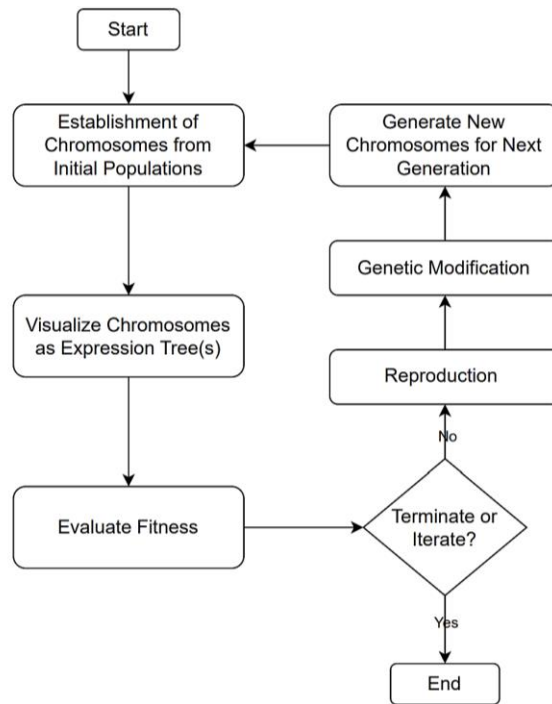
Figure 2. GEP algorithm flowchart of SCWBs

Table 3. Results of various gene models investigated during the optimization stage

Models Set	Chromosomes	Head Size	Number of Genes	Linking Function	Testing R^2
GEP1	50	8	4	Addition	0.88
GEP2	50	8	3	Addition	0.82
GEP3	50	10	3	Addition	0.78
GEP4	50	12	3	Addition	0.75
GEP5	100	9	3	Addition	0.73
GEP6	100	14	4	Addition	0.91
GEP6	100	14	4	Multiplication	0.86
GEP7	100	8	3	Addition	0.85
GEP8	100	12	4	Addition	0.91
GEP9	100	12	3	Addition	0.83
GEP10	150	8	3	Addition	0.78
GEP11	150	12	4	Addition	0.77
GEP12	150	10	4	Addition	0.85
GEP13	150	12	4	Multiplication	95
GEP14	150	8	3	Multiplication	0.82
GEP15	150	9	3	Addition	0.81
GEP16	100	10	3	Addition	0.8
GEP17	150	12	4	Addition	0.84
GEP18	150	9	3	Multiplication	0.85
GEP19	100	10	3	Addition	0.79

3.4. Performance Assessment Metrics

This study used several performance metrics to assess the accuracy of the developed machine-learning models. These models are coefficient of determination (R^2) (Equation 1), root-mean-square error (RMSE) (Equation 2), and mean absolute error (MAE) (Equation 3).

$$R^2 = 1 - \frac{\sum(y_i - \hat{y}_i)^2}{\sum(y_i - \bar{y})^2} \tag{7}$$

$$\text{RMSE} = \sqrt{\frac{\sum_{i=1}^{n}(y_i - \hat{y}_i)^2}{n}} \tag{8}$$

$$\text{MAE} = \frac{1}{n}\sum_{i=1}^{n}|y_i - \hat{y}_i| \tag{9}$$

where y_i is the actual value, $\hat{y}_i$ is the predicted one, $\bar{y}$ is the average of the measured values, and n is the number of observations.

4. Results and Discussions

4.1. Shear Capacity Estimation Using Gene Expression Programming

The GEP model 13, shown in Figure 3 and explained using Table 4, is used as an advanced machine learning technique and shows remarkable performance in predicting the shear strength of Sinusoidal steel corrugated web beams (SCWB). The evaluation of its effectiveness shown in Table 5, as indicated by the performance metrics, reveals its substantial predictive accuracy and reliability. In the validation phase, the model achieved a root mean square error (RMSE) of 76.5 and a mean absolute error (MAE) of 64.3. These metrics suggest that the GEP model can predict with a high degree of precision, with minimal deviation from the actual values. More impressively, the model attained an R^2 score of 0.97. Transitioning to the testing phase, the GEP model maintained a commendable level of performance, with an RMSE of 100.5 and an MAE of 86.6. While these values are slightly higher than those in the validation phase, they still underscore the model's ability to handle new, unseen data effectively. The R^2 value of 0.95 in the testing phase further confirms the model's robustness, demonstrating its capacity to capture a significant proportion of the variability in the test data. Figure 4 shows the mode performance compared with the actual data. When compared with other machine learning models tested for the same purpose, the GEP model stands out for its high R^2 values in both validation and testing phases. While there is an increase in error metrics (RMSE and MAE) in the test phase, it still maintains an accurate predictive performance. The model's slight decrease in precision with new data suggests an area for further optimization, possibly through fine-tuning of its parameters or more comprehensive training with diverse datasets.

Table 4. GEP regression function definitions

Function	Representation	Definition
Addition	+	(x+y)
Subtraction	-	(x-y)
Multiplication	*	(x×y)
Division	/	(x/y)
Exponential	*Exp*	*exp(x)*
Natural logarithm	*Ln*	*In(x)*
Inverse	*Inv*	*1/x*
x to the power of 2	*x²*	*x²*
Cube root	*3Rt*	*x^{1/3}*
Minimum of 2 inputs	*Min2*	*min(x,y)*
Maximum of 2 inputs	*Max2*	*max(x,y)*
Average of 2 inputs	*Avg2*	*avg(x,y)*
Arctangent	*Atan*	*arctan(x)*
Hyperbolic tangent	*Tanh*	*tanh(x)*
Complement	*NOT*	*(1-x)*
constant	*C*	*c1,c2,c3,....*

Table 5. Performance assessment of the GEP model

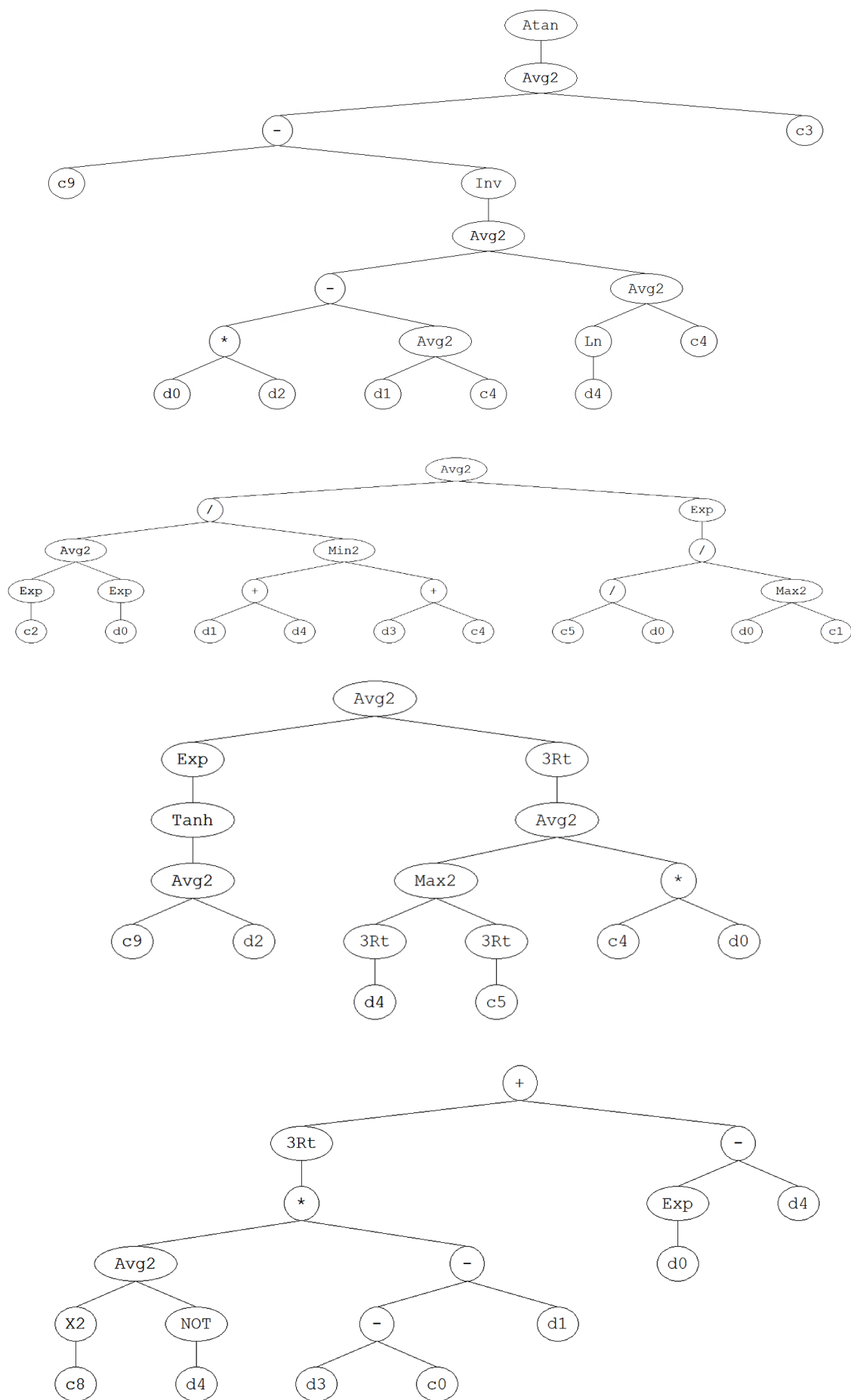| Model Type	Gene Expression Programming
RMSE (Validation)	76.5
R^2 (Validation)	0.97
MAE (Validation)	64.3
RMSE (Test)	100.5
R^2 (Test)	0.95
MAE (Test)	86.6

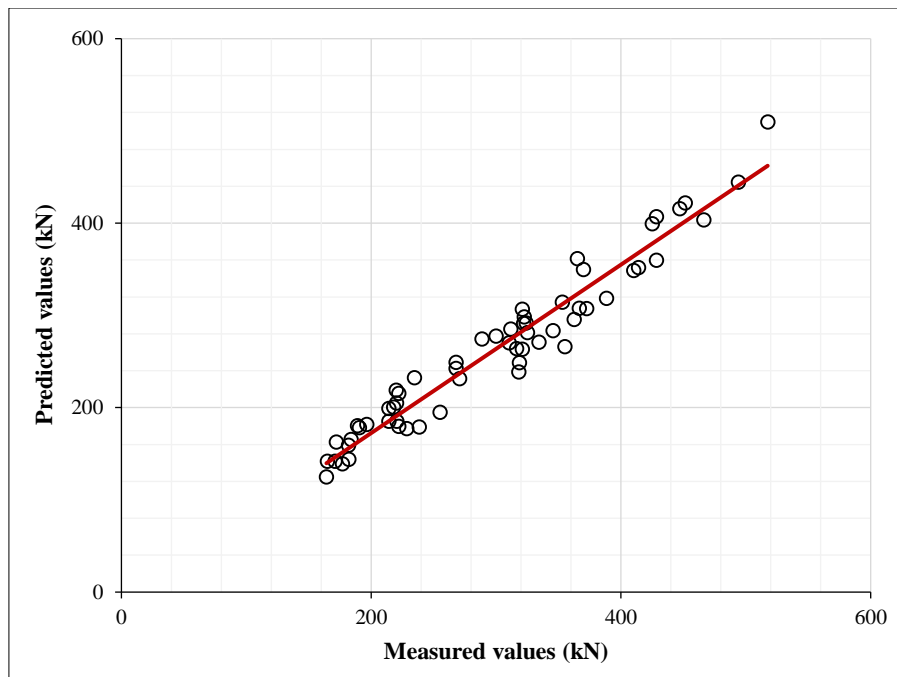**Figure 3. Developed GEP model for SCWB's shear prediction**

Figure 4. Shear capacity estimation using the GEP approach

4.2. Comparison Against Commonly Used Models

Three commonly used machine learning techniques were examined to predict the shear strength of SCWB to compare the performance of the optimized GEP model. These models are linear regression with robust linear preset, quadratic support vector machine (SVM), and optimizable neural network. The performance of the models against that of the GEP is given in Figure 5 to Figure 7. It can be seen that the linear regression model featuring a robust linear preset has reached an RMSE of 55.46, an R^2 of 0.72, and an MAE of 37.516 for the validation dataset. The Quadratic SVM utilized a quadratic kernel function with standardized data, achieving an RMSE of 56.15, an R^2 of 0.71, and an MAE of 38.9 for validation. The optimizable neural network, standardized with a preset single fully connected layer of size 99 and ReLU activation, achieved an RMSE of 54.45, an R^2 of 0.73, and an MAE of 39.37 for the validation dataset. While the optimizable neural network slightly outperformed the other models based on RMSE, R^2, and MAE for the validation dataset, it demanded a notably longer training duration. On the other hand, it can be seen that the proposed GEP model provides the best results against other techniques.
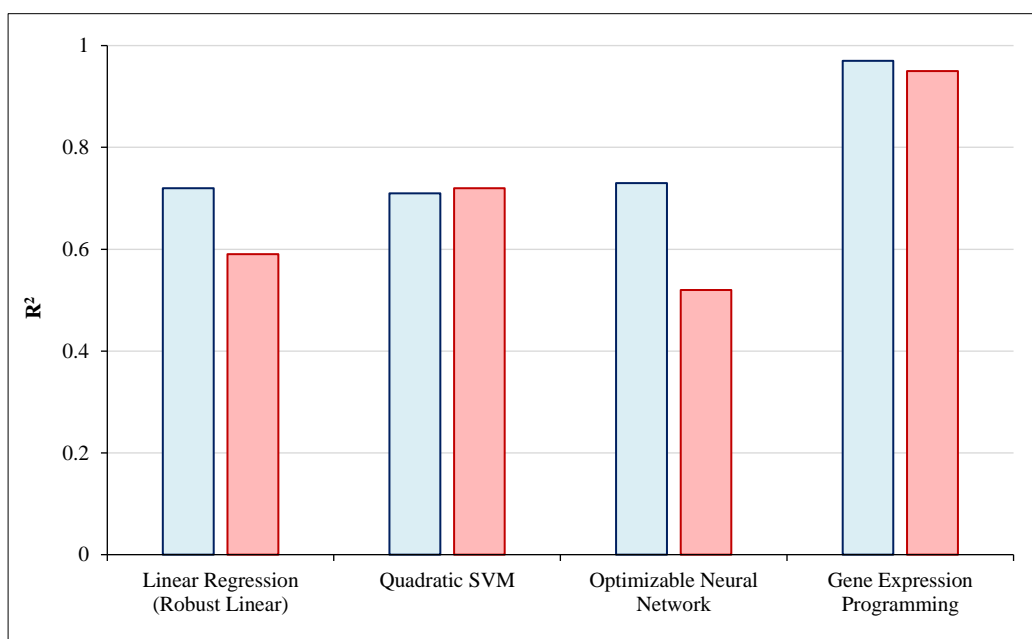

Figure 5. Benchmarking the R^2 value of GPE model against commonly used techniques for predicting shear strength of SCWB
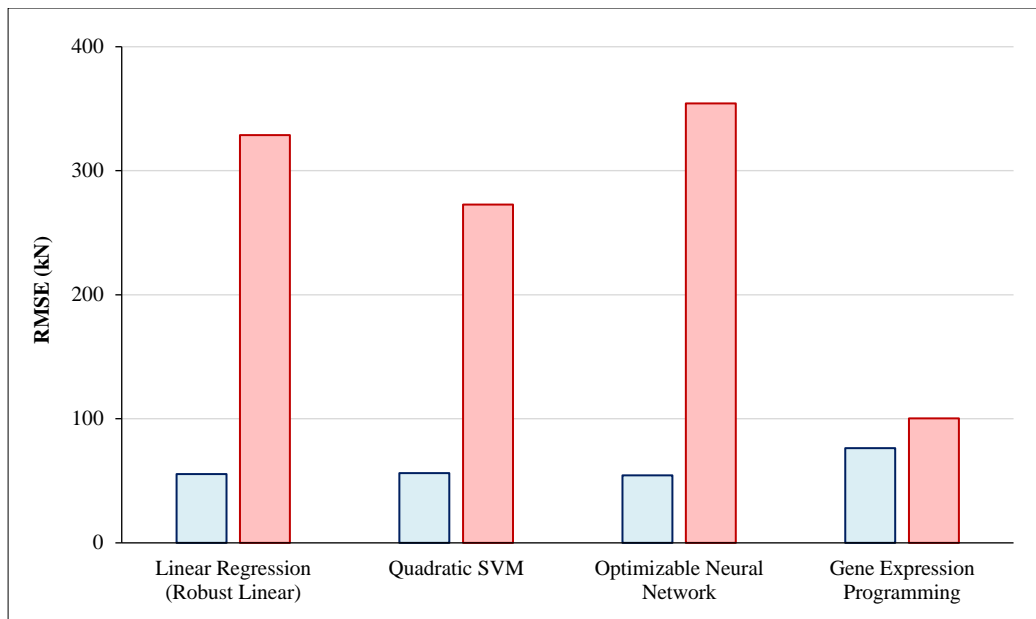
Figure 6. Benchmarking the RMSE value of GPE model against commonly used techniques for predicting shear strength of SCWB
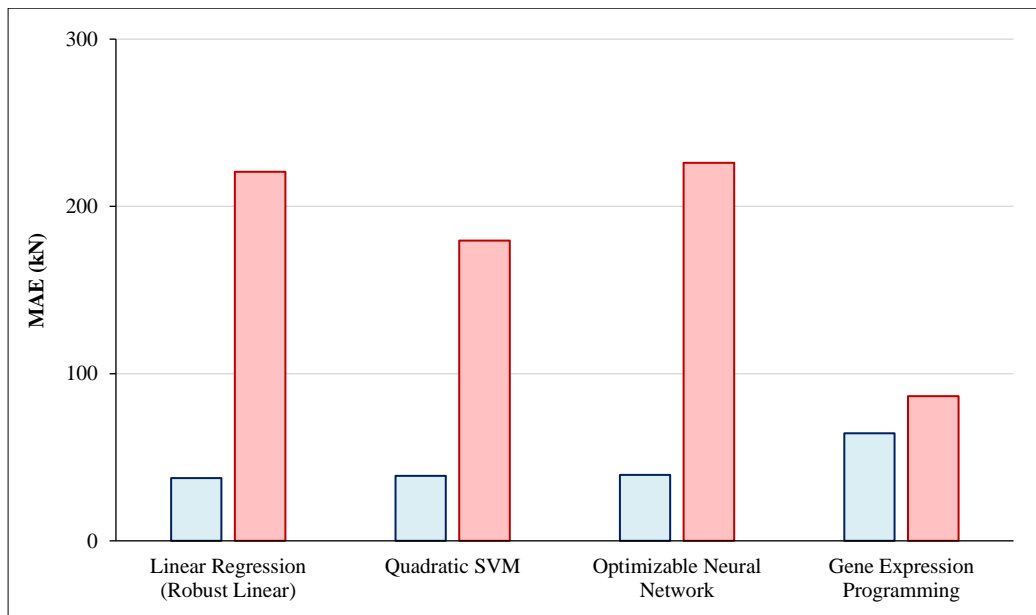

Figure 7. Benchmarking the MAE value of the GPE model against commonly used techniques for predicting the shear strength of SCWB

4.3. Variable Importance and Sensitivity Analysis

This section evaluates the influence of various parameters on the shear strength of SCWB. This investigation aims to understand the relative influence exerted by various structural parameters on the shear strength of SCWB. The methodology employed an extensive sensitivity analysis and F-test variable importance analysis, as shown in Figures 8 and 9. The web depth (h_w) of sinusoidal corrugated steel webs is the most influential parameter in determining shear strength, as evidenced by its highest variable importance score of 1.2 in the GEP 13 model analysis. This significance is reflected in the sensitivity analysis, where variations in h_w lead to noticeable changes in shear strength. This highlights the critical role of web depth in the structural stability and load-bearing capacity of corrugated steel webs, making it a critical factor in design considerations and structural assessments. Web thickness (t_w) demonstrates a substantial impact on the shear strength of sinusoidal corrugated steel webs, albeit less than web depth, with a variable importance score of 0.5. The sensitivity analysis likely indicates noticeable changes in shear strength with variations in t_w, though these changes are not as steep as those observed for h_w. The moderate yet significant influence of web thickness highlights its role in the overall structural behavior of corrugated steel webs, compelling careful consideration in design to optimize performance.

The corrugation depth (a_3) holds a notable position in influencing the shear strength of sinusoidal corrugated steel webs, as indicated by its variable importance score of 0.4. This score suggests that a3 is a key structural element, with its depth playing an integral role in imposing the web's behavior under load. The sensitivity analysis for a_3 likely reveals significant shifts in shear strength in response to changes in corrugation depth, suggesting that deeper corrugations might incrementally enhance the structural performance of SCWB designs up to a certain limit where the effect of the a_3 become stable and no longer affect the shear strength. The wavelength of the sinusoidal panel (a_1) presents a lower importance means of 0.25. The sensitivity analysis for a1 exhibits an inverse relationship with shear strength. This finding aligns with previous studies indicating that larger longitudinal fold panels reduce shear strength, potentially due to increased flexibility or stress concentrations [42, 43]. The steel yield strength (τ_y) shows the least impact on the shear strength of sinusoidal corrugated steel webs within the parameter range studied, as evidenced by its low variable importance score of 0.02. The sensitivity analysis for τ_y likely displays minimal fluctuations in shear strength, suggesting that, within the studied context, variations in the steel's yield strength are less influential compared to other geometric factors. This observation points to the dominant role of structural geometry over material properties in determining the performance of corrugated steel webs in this specific analysis.
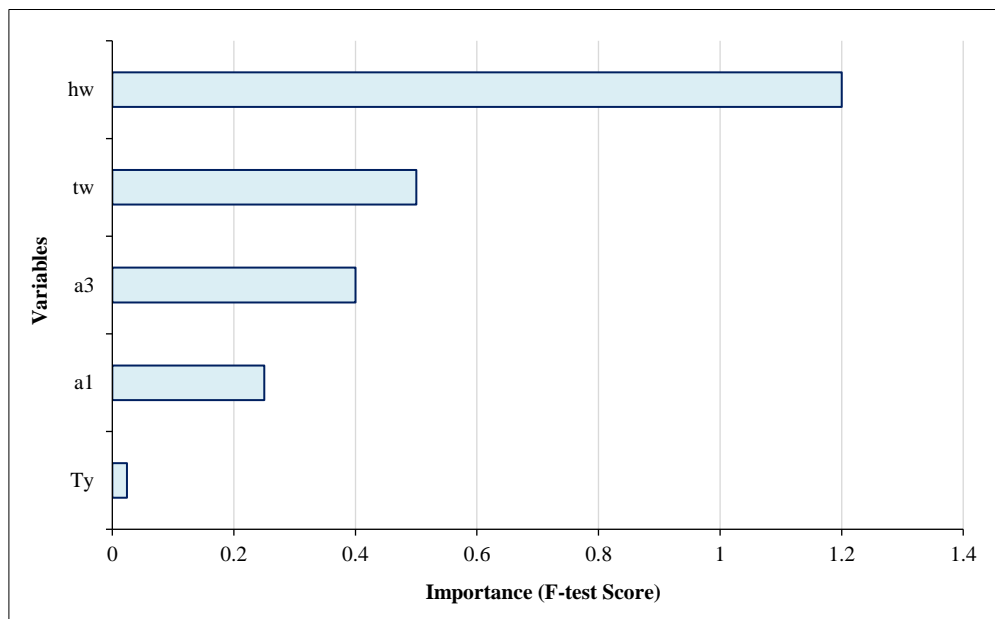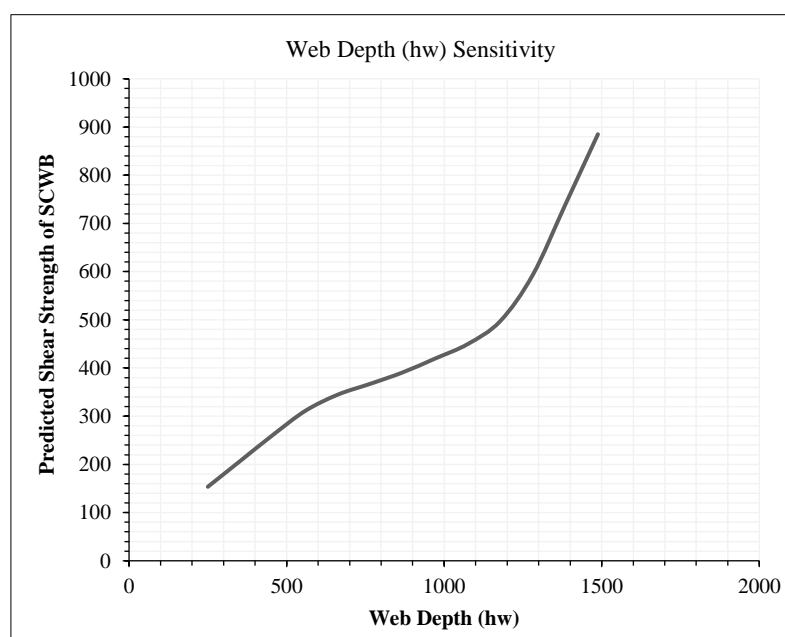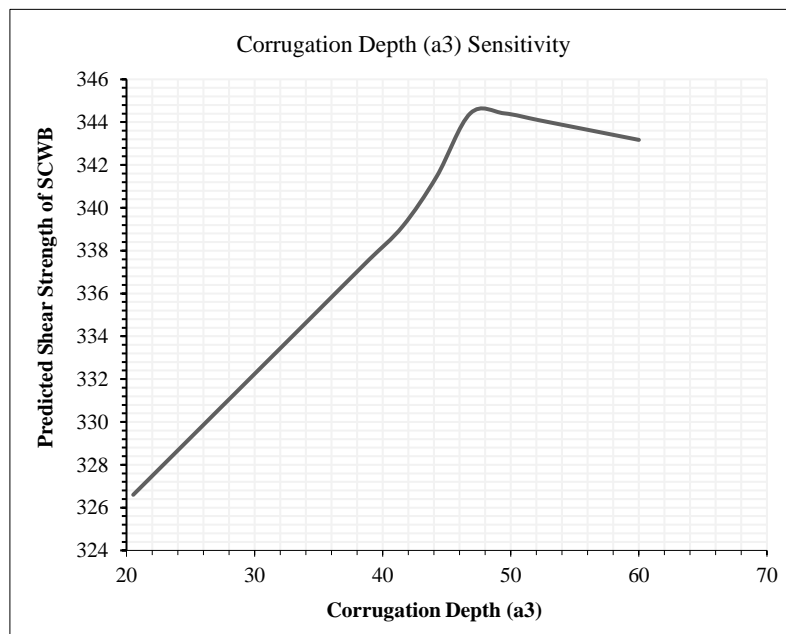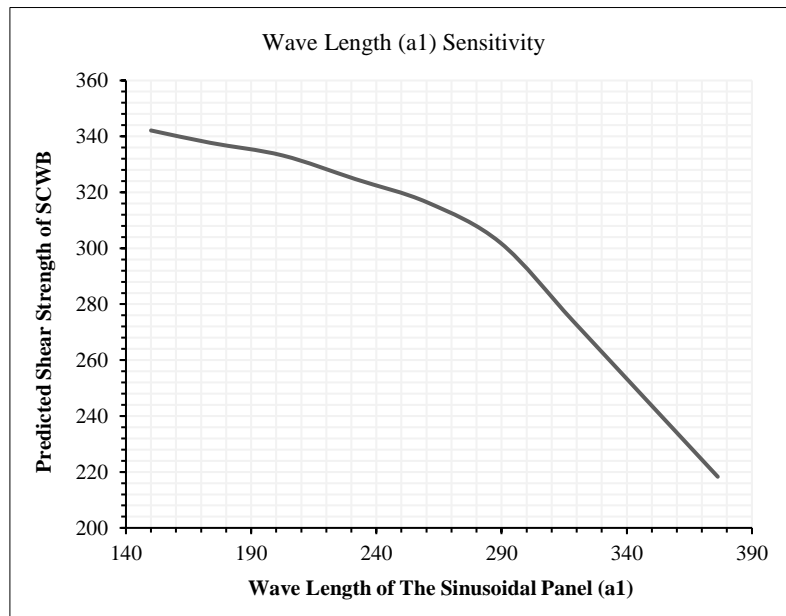

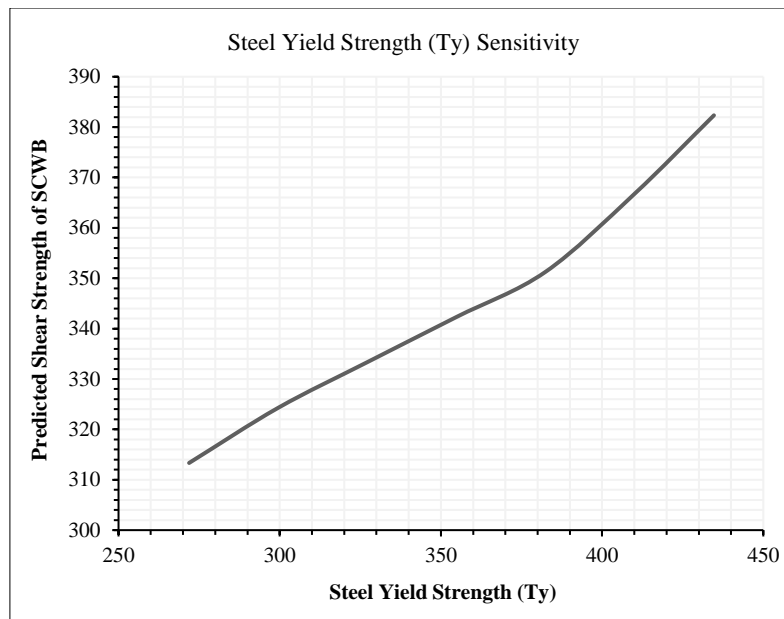**Figure 8. F-test Importance of features for shear strength determination in SCWB**

Web Thickness (tw) Sensitivity

Wave Length (a1) Sensitivity

Corrugation Depth (a3) Sensitivity
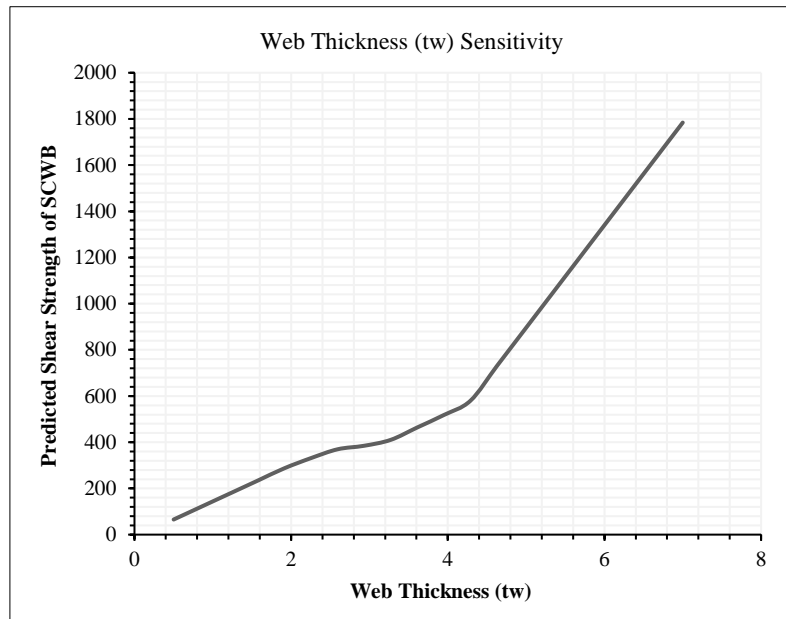
Figure 9. GEP model analysis of shear strength changes across sinusoidal configuration parameters

5. Conclusions

In this research, the application of GEP for predicting the shear capacity of SCWBs was thoroughly investigated. The developed GEP model demonstrated high predictive accuracy, with an RMSE of 100.5, an MAE of 86.6, and an impressive R^2 value of 0.95, indicating robustness and reliability in predictions. Through parametric analysis, the statistical properties of the data were assessed, and the influence of various parameters on the shear strength of SCWBs was evaluated. The optimized model achieved commendable results in handling new data and highlighted the influence of structural parameters such as web height and thickness on SCWB strength. The parametric analysis assessed these parameters' statistical properties and sensitivities, reinforcing GEP's ability to capture complex relationships within structural elements.

Key highlights from the study include:

- Optimized GEP Model: GEP13 was the most effective model, combining 150 chromosomes, a head size 12, and a multiplication linking function, achieving an R^2 of 0.95.

- Predictive Accuracy: The model demonstrated high predictive accuracy in both the validation and testing phases, with robustness in handling new, unseen data.

- Parameter Influence: Detailed parametric analysis revealed significant influences of web height (h_w) and thickness (t_w) on shear strength, which is critical for design considerations. These findings align closely with recent experimental studies and observed mechanical behavior.

- Comparative Analysis: Compared to other machine learning techniques like linear regression and support vector machines, GEP provided superior results, highlighting its suitability for complex structural predictions.

The high predictive accuracy, combined with a detailed evaluation of parameter influence, underscores the significant potential of GEP as a tool in structural engineering. This study affirms the high capability of gene expression programming in structural predictions and lays a substantial groundwork for future advancements in predictive modeling techniques for evaluating structural elements, further enriching the field of structural engineering with robust, reliable modeling tools.

6. Nomenclatures

m	Number of corrugations	h_r, a_3	Corrugation depth
h_w	Web depth	L	Web length
t	Web thickness	w_2	Smaller values of b and c
w	Larger values of b and c	w_2/w	Fold ratio
E	Young's modulus of elasticity	τ_y	Yield shear stress
f_y	Yield tensile stress	τ_u	Ultimate shear stress, $\tau_u = Q_u/(h_t)$
τ_{Lel}	Local elastic shear buckling stress	τ_{Iel}	Interactive elastic shear buckling stress

τ_{Gel}	Global elastic shear buckling stress	$\tau_{cr,L}$	Critical local shear buckling stress
$\tau_{cr,G}$	Critical global shear buckling stress	k_{Lel}	Local shear buckling stress buckling coefficient
$\tau_{cr,I}$	Critical interactive shear buckling stress	k_G	Global shear buckling stress buckling coefficient
ρ_L	Normalized local elastic shear buckling strength	$\rho_{I,n,el}$	Normalized interaction elastic shear buckling strength
ρ_G	Normalized global elastic shear buckling strength		

7. Declarations

7.1. Author Contributions

Conceptualization, M.S., Z.A., and S.B.; methodology, M.S., Z.A., S.B., A.H., and O.M.; formal analysis, M.S., Z.A., S.B., A.H., and O.M.; investigation, M.S., Z.A., S.B., A.H., and O.M.; writing—original draft preparation, M. S., Z.A., A.H., and O.M.; writing—review and editing, Z.A. and S. B.; supervision, Z.A. and S.B. All authors have read and agreed to the published version of the manuscript.

7.2. Data Availability Statement

The data presented in this study are available as an appendix in this article.

7.3. Funding

The authors received no financial support for the research, authorship, and/or publication of this article.

7.4. Conflicts of Interest

The authors declare no conflict of interest.

8. References

[1] Ou, X., Liao, L., Lyu, X., & Qiao, Y. (2023). Numerical analysis and parameter optimization of corrugated steel web. Advances in Frontier Research on Engineering Structures, CRC Press, Boca Raton, United States. doi:10.1201/9781003363217-57.

[2] Tetougueni, C. D., Maiorana, E., Zampieri, P., & Pellegrino, C. (2019). Plate girders behavior under in-plane loading: A review. Engineering Failure Analysis, 95, 332–358. doi:10.1016/j.engfailanal.2018.09.021.

[3] Leblouba, M., Karzad, A. S., Tabsh, S. W., & Barakat, S. (2022). Plated versus Corrugated Web Steel Girders in Shear: Behavior, Parametric Analysis, and Reliability-Based Design Optimization. Buildings, 12(12). doi:10.3390/buildings12122046.

[4] Hassanein, M. F., Zhang, Y. M., Elkawas, A. A., Al-Emrani, M., & Shao, Y. B. (2022). Small-scale laterally-unrestrained corrugated web girders: (II) Parametric studies and LTB design. Thin-Walled Structures, 180. doi:10.1016/j.tws.2022.109776.

[5] Papangelis, J., Trahair, N., & Hancock, G. (2017). Direct strength method for shear capacity of beams with corrugated webs. Journal of Constructional Steel Research, 137, 152–160. doi:10.1016/j.jcsr.2017.06.007.

[6] Giglioni, V., Venanzi, I., & Ubertini, F. (2023). Supervised machine learning techniques for predicting multiple damage classes in bridges. Sensors and Smart Structures Technologies for Civil, Mechanical, and Aerospace Systems 2023. doi:10.1117/12.2664359.

[7] Barkhordari, M. S., & Jawdhari, A. (2023). Machine learning based prediction model for plastic hinge length calculation of reinforced concrete structural walls. Advances in Structural Engineering, 26(9), 1714–1734. doi:10.1177/13694332231174252.

[8] Markou, G., Bakas, N., & Megan van der Westhuizen, A. (2023). Use of AI and ML Algorithms in Developing Closed-Form Formulae for Structural Engineering Design. Artificial Intelligence and Machine Learning Techniques for Civil Engineering, 73–105. doi:10.4018/978-1-6684-5643-9.ch004.

[9] Noori Hoshyar, A., Rashidi, M., Yu, Y., & Samali, B. (2023). Proposed Machine Learning Techniques for Bridge Structural Health Monitoring: A Laboratory Study. Remote Sensing, 15(8), 1984. doi:10.3390/rs15081984.

[10] Gottardi, N., Freitag, S., & Meschke, G. (2023). Structural stress prediction based on deformations using artificial neural networks trained with artificial noise. PAMM, 22(1), e202200035. doi:10.1002/pamm.202200035.

[11] Alotaibi, E., Mostafa, O., Nassif, N., Omar, M., & Arab, M. G. (2021). Prediction of Punching Shear Capacity for Fiber-Reinforced Concrete Slabs Using Neuro-Nomographs Constructed by Machine Learning. Journal of Structural Engineering, 147(6), 04021075. doi:10.1061/(asce)st.1943-541x.0003041.

[12] Mostafa, O., Alotaibi, E., Al-Ateyat, A., Nassif, N., & Barakat, S. (2022). Prediction of Punching Shear Capacity for Fiber-Reinforced Polymer Concrete Slabs Using Machine Learning. 2022 Advances in Science and Engineering Technology International Conferences (ASET), Dubai, United Arab Emirates. doi:10.1109/aset53988.2022.9735107.

[13] Elamary, A. S., & Taha, I. B. M. (2021). Determining the shear capacity of steel beams with corrugated webs by using optimised regression learner techniques. Materials, 14(9), 2364. doi:10.3390/ma14092364.

[14] İpek, S., Degtyarev, V. V., Güneyisi, E. M., & Mansouri, I. (2022). GEP-based models for estimating the elastic shear buckling and ultimate loads of cold-formed steel channels with staggered slotted web perforations in shear. Structures, 46, 186–200. doi:10.1016/j.istruc.2022.10.060.

[15] Hossain, M. A. S., Uddin, M. N., & Hossain, M. M. (2023). Prediction of compressive strength fiber-reinforced geopolymer concrete (FRGC) using gene expression programming (GEP). Materials Today: Proceedings. doi:10.1016/j.matpr.2023.02.458.

[16] Alabduljabbar, H., Khan, M., Awan, H. H., Eldin, S. M., Alyousef, R., & Mohamed, A. M. (2023). Predicting ultra-high-performance concrete compressive strength using gene expression programming method. Case Studies in Construction Materials, 18. doi:10.1016/j.cscm.2023.e02074.

[17] Wang, T., Ma, J., & Wang, Y. (2021). Normalized shear strength of trapezoidal corrugated steel web dominated by local buckling. Engineering Structures, 233. doi:10.1016/j.engstruct.2021.111909.

[18] Johansson, B., Maquoi, R., Sedlacek, G., Müller, C., & Beg, D. (2007). Commentary and worked examples to EN 1993-1-5 Plated Structural Elements. JRC scientific and technical reports, European Commissions, Brussels, Belgium.

[19] Easley, J. T. (1975). Buckling Formulas for Corrugated Metal Shear Diaphragms. Journal of the Structural Division, 101(7), 1403–1417. doi:10.1061/jsdeag.0004095.

[20] Easley, J. T., & McFarland, D. E. (1969). Buckling of Light-Gage Corrugated Metal Shear Diaphragms. Journal of the Structural Division, 95(7), 1497–1516. doi:10.1061/jsdeag.0002313.

[21] Nikoomanesh, M. R., & Goudarzi, M. A. (2020). Experimental and numerical evaluation of shear load capacity for sinusoidal corrugated web girders. Thin-Walled Structures, 153. doi:10.1016/j.tws.2020.106798.

[22] Pasternak, H., & Branka, P. (1999). Load-bearing behavior of corrugated web girders under local load application. Bauingenieur 74, 5(5), 219–244.

[23] Elkawas, A. A., Hassanein, M. F., & El-Boghdadi, M. H. (2017). Numerical investigation on the nonlinear shear behavior of high-strength steel tapered corrugated web bridge girders. Engineering Structures, 134, 358–375. doi:10.1016/j.engstruct.2016.12.044.

[24] Hajdú, G., Pasternak, H., & Papp, F. (2023). Lateral-torsional buckling assessment of I-beams with sinusoidally corrugated web. Journal of Constructional Steel Research, 207, 107916. doi:10.1016/j.jcsr.2023.107916.

[25] Friedberg, R. M. (2010). A Learning Machine: Part I. IBM Journal of Research and Development, 2(1), 2–13. doi:10.1147/rd.21.0002.

[26] Ferreira, C. (2001). Gene expression programming: a new adaptive algorithm for solving problems. arXiv preprint cs/0102027. doi:10.48550/arXiv.cs/0102027.

[27] Holland, J. H. (1975). Adaptation in Natural and Artificial Systems. The University of Michigan Press, Ann Arbor, United States.

[28] Cramer, N. L. (2014). A representation for the adaptive generation of simple sequential programs. Proceedings of the First International Conference on Genetic Algorithms and Their Applications, 240. doi:10.4324/9781315799674.

[29] Koza, J. R. (1992). Genetic programming: on the programming of computers by means of natural selection. Bradford, Denver, United States.

[30] Ferreira, C. (2006). Gene expression programming: mathematical modeling by an artificial intelligence. Springer, Berlin, Germany. doi:10.1007/3-540-32849-1.

[31] Faessler, E., Hahn, U., & Schauble, S. (2023). GePI: Large-scale text mining, customized retrieval and flexible filtering of gene/protein interactions. Nucleic Acids Research, 51(W1), W237–W242. doi:10.1093/nar/gkad445.

[32] Kontoni, D. P. N., Onyelowe, K. C., Ebid, A. M., Jahangir, H., Rezazadeh Eidgahee, D., Soleymani, A., & Ikpa, C. (2022). Gene Expression Programming (GEP) Modelling of Sustainable Building Materials including Mineral Admixtures for Novel Solutions. Mining, 2(4), 629–653. doi:10.3390/mining2040034.

[33] Anas, M., Khan, M., & Basit, H. (2021). A Comparative Study on the Performance of Gene Expression Programming and Machine Learning Methods. International Journal of Scientific Research in Science and Technology, 8(2), 140–147. doi:10.32628/ijsrset1218226.

[34] SIN Beam Technical Guide (2018). Corrugated Web Steel Beam: STEELCON Fabrication Inc. Ontario, Canada, 1-141

[35] Pasternak, H., & Kubieniec, G. (2011). Present state of art of plate girders with sinusoidally corrugated web. In Proceedings of the 10th International Conference on Steel Space and Composite Structures, 1-15.

[36] Śledziewski, K., & Górecki, M. (2020). Finite element analysis of the stability of a sinusoidal web in steel and composite steel-concrete girders. Materials, 13(5), 1041. doi:10.3390/ma13051041.

[37] Górecki, M., & Śledziewski, K. (2022). Influence of corrugated web geometry on mechanical properties of I-beam: Laboratory tests. Materials, 15(1), 277. doi:10.3390/ma15010277.

[38] Hannebauer, D. (2007). On the cross-sectional and bar load-bearing capacity of beams with profiled webs. Ph.D. Thesis, BTU Cottbus-Senftenberg, Cottbus, Germany. (In German).

[39] Basiński, W. (2018). Shear Buckling of Plate Girders with Corrugated Web Restrained by End Stiffeners. Periodica Polytechnica Civil Engineering, 1-15. doi:10.3311/ppci.11554.

[40] Yan-Lin, G., Qing-Lin, Z., Siokola, W., & Andreas, H. (2008). Flange buckling behavior of the H-shaped member with sinusoidal webs. Fifth International Conference on Thin-Walled Structures, 18-20 June, 2008, Gold Coast, Australia.

[41] Nikoomanesh, M. R., & Goudarzi, M. A. (2021). Patch loading capacity for sinusoidal corrugated web girders. Thin-Walled Structures, 169, 108445. doi:10.1016/j.tws.2021.108445.

[42] Abdullah, M. D., & Almayah, A. A. (2023). The Effect of Shear Span on the Behavior of Triangularly Corrugated Web Steel Girders. Civil Engineering Journal (Iran), 9(2), 372–380. doi:10.28991/CEJ-2023-09-02-09.

[43] Wang, P. Y., Garlock, M. E. M., Zoli, T. P., & Quiel, S. E. (2021). Low-frequency sinusoids for enhanced shear buckling performance of thin plates. Journal of Constructional Steel Research, 177. doi:10.1016/j.jcsr.2020.106475.

Appendix I

Table A1. Collected database in this study

h_w	t_w	τ_y	a_1	a_3	V_u	h_w	t_w	τ_y	a_1	a_3	V_u
500	2.5	224.9357	155	40	288.69	500	2	175.7454	156	40	165
500	2.5	224.9357	155	40	316.27	500	2.6	159.2909	156	40	218
500	2.5	224.9357	155	40	311.82	1000	2.5	150.342	156	40	362.5
1000	2	241.6211	155	40	345.63	1000	2.6	183.4819	156	40	372.5
1000	2	241.6211	155	40	366.53	1250	2	142.721	156	40	425
1000	2	241.6211	155	40	354.97	1500	2	153.6906	156	40	414
1502	2.1	129.9038	155	40	370	1000	2	193.0082	156	40	310.5
1501	2.1	129.9038	155	40	365	1000	2.5	196.761	156	40	447
1505	2.1	129.9038	155	40	353	1000	3	187.9275	156	40	517.5
500	2.1	177.2465	155	40	177	1500	2	167.0274	156	40	428.5
500	2.1	181.288	155	40	182	500	2	173.2051	306.8	20	190.5
500	2	174.3598	155	40	171	500	2.5	173.2051	306.8	20	238.5
500	2.1	171.473	155	40	172	750	2.5	173.2051	306.8	20	324
350	7	250.57	150	25	1360.49	750	3	173.2051	306.8	20	388.5
350	7	250.57	150	25	1611.28	1000	2.5	173.2051	306.8	20	428.5
500	3	204.9593	155	43	322	1000	3	173.2051	306.8	20	494
500	3	204.9593	155	43	255	501	2.6	132.7906	345.8	39.3	220.5
500	3	204.9593	155	43	189	501	2.6	132.7906	345.8	39.2	220.25
500	3	204.9593	155	43	125	500	2.6	132.7906	345.8	39.3	222
500	2	204.9593	155	43	214	502	2.6	132.7906	345.8	39.1	228.5
500	2	204.9593	155	43	214	500	2	174.3598	159.2	38	322.5
500	2.5	204.9593	155	43	268	500	2	174.3598	159.2	38	318.75
500	2.5	204.9593	155	43	268	500	2	174.3598	159.2	38	318.25
500	3	204.9593	155	43	321	750	2.5	132	213	60	270.66
500	3	204.9593	155	43	321	500	3	137	213	60	234.67
250	3	204.9593	155	43	183.86	750	3	137	213	60	300.08
250	3	204.9593	155	43	181.8	500	4	140	213	60	334.41
250	3	204.9593	200	55	196.51	625	4	140	213	60	410.11
250	5	204.9593	200	55	289.43	750	4	140	213	60	466.31
250	3	204.9593	381	140	164.17	330	5	143	213	60	325.09
250	5	204.9593	381	140	236.61	500	5	143	213	60	451.4
500	2.5	132.7906	155	40	220	625	5	143	213	60	590.07
500	2.5	132.7906	155	40	222						